

Impact of $f(\mathcal{Q})$ Theory on the Stability of Compact Spherical Solutions

Shamaila Rani ^{1,2} ^{*}; Muhammad Adeel ² [†]; M. Zeeshan Gul ^{3,4} [‡];
 and Abdul Jawad ^{1,2} [§] Institute for Theoretical Physics and Cosmology,
 Zhejiang University of Technology, Hangzhou 310023, China
² Department of Mathematics, COMSATS University Islamabad,
 Lahore-Campus, Lahore-54000, Pakistan.
³ Department of Mathematics and Statistics, The University
 of Lahore 54792, Pakistan.
⁴ Research Center of Astrophysics and Cosmology, Khazar University,
 Baku, AZ1096, 41 Mehseti Street, Azerbaijan.

Abstract

This research paper examines the feasibility and stability of compact stars in the context of $f(\mathcal{Q})$ theory, where \mathcal{Q} represents the non-metricity scalar. To achieve this objective, a static spherical line element is assumed in the interior region and the Schwarzschild spacetime is used in the exterior region of the star. The unknown constants are determined by using the Darmois junction conditions. We consider a specific model of this theory to investigate the viability of compact stars through various physical quantities such as matter contents, energy bounds, anisotropy and state parameters. The stability states for the stellar objects under consideration are determined by the speed

^{*}shamailatoor.math@yahoo.com; drshamailarani@cuilahore.edu.pk

[†]mr.adimaths@gmail.com

[‡]mzeeshangul.math@gmail.com

[§]jawadab181@yahoo.com; abduljawad@cuilahore.edu.pk

of sound and adiabatic index, respectively. The resulting data indicate that the compact stars in this modified framework are physically viable and stable.

Keywords: Modified gravitational theory; Stellar structures; Stability analysis.

PACS: 98.35.Ac; 98.80.Jk; 04.50.Kd; 04.40.Dg.

1 Introduction

The recent advancements in gravitational physics and cosmic science have brought significant attention to the rapid expansion of the universe [1]-[2]. These developments have provided new insights into understanding the fundamental and practical modifications that contribute to the rapid growth of galaxies. Many results have provided strong evidence to understand the expansion of the universe [3]-[5]. The universe is expanding faster than ever before due to an unknown factor known as dark energy. Moreover, it is estimated that 68 percent of total energy is unexplained in the form of DE. Therefore, researchers need to make some modifications to the general theory of relativity (GR) to determine the cosmic expansion. These kinds of studies encourage researchers to investigate viable modifications or extensions of gravity theories that could simulate the situations when the GR yields unfavorable results. Cosmologists have explored some alternative gravitational theories in response to the limitations of GR. There are different forms of modified theories such as curvature, torsion and non-metricity-based theories [6]-[17].

Modified theories of gravity successfully offer the alternative explanations to GR by addressing unsolved issues of the universe. Recently, extensive research has delved into the implications of modified theories. Weyl in his work [18] integrated electromagnetic and gravitational forces into a more generic geometry by introducing the concept of non-metricity (covariant divergence is zero for metric tensor). Cartan [19] developed the Einstein-Cartan theory by extending GR in the presence of torsion field. Weitzenbock space [20] features zero curvature and torsion replaces curvature in teleparallel theory. Introduction of non-metric variables such as the non-metricity in symmetric teleparallel gravity, further refines this framework. Notably, both torsion and curvature remain zero in this formulation.

The $f(\mathcal{Q})$ theory explores an alternative route where non-metricity is the driving factor, capturing considerable attention among researchers due to its profound implications in gravitational physics. The exploration of this theory is motivated by a desire to understand its theoretical implications and significance in astrophysical as well as cosmological contexts. In $f(\mathcal{Q})$ theory, the inclusion of non-metricity enables a more detailed depiction of gravitational interactions. Non-metricity represents the deviation from the Levi-Civita connection, which is the connection compatible with the metric tensor in GR. By incorporating non-metricity into the gravitational action, this theory introduces additional degrees of freedom, leading to new gravitational dynamics and cosmological solutions. This modification influences the internal structure of pulsars, leading to alterations in the pressure-density relationship and changes in stellar radii and mass profiles. Consequently, the equations of motion derived from this theory impact the hydrostatic equilibrium and stability of stars. Neutron stars serve as prime sources of gravitational waves which exhibit distinct signatures under the influence of $f(\mathcal{Q})$ gravity, differing from those predicted by GR. Noteworthy, outcomes highlight the presence of additional correction terms, potentially influencing the geometric viability when compared to GR. The exploration of this theory is motivated by a desire to understand its theoretical implications and significance in astrophysical as well as cosmological contexts.

The non-metricity is a mathematical concept that emerges in theories involving non-Riemannian geometries, providing an alternative cosmic model without dark energy. Researchers are drawn to explore non-Riemannian geometry, specifically $f(\mathcal{Q})$ theory, for various reasons such as its theoretical implications, compatibility with observational data and its significance in cosmological contexts [21]. Recent investigations into $f(\mathcal{Q})$ gravity have revealed cosmic issues and observational constraints can be employed to indicate deviations from the Λ CDM model [22]. Spherical symmetric configurations in $f(\mathcal{Q})$ gravity have been analyzed in [23]. Ambrosio [24] described perturbation corrections to the Schwarzschild solution in the same theory. Ambrosio et al [25] delved into the asymptotic behavior of Schwarzschild-like solutions in $f(\mathcal{Q})$ theory. The non-metricity scalar has been employed to detect the effects of microscopic systems in [26]. The viable cosmological solutions in symmetric teleparallel gravity through the Noether symmetry technique have been explored in [27]. Barros et al [28] analyzed the cosmic characteristics through redshift space distortion data in non-metricity gravity. This modified theory can elucidate the cosmic bounce scenario [29] and describes dark

energy features at large scales [30]. For further details, we refer the readers to [31]-[36].

Adak [37] studied the symmetric teleparallel gravity model in which only non-metricity is non-zero. They obtained a spherically symmetric static solution to Einstein equation in symmetric teleparallel gravity and discussed the singularities. Nester and Yo [38] studied teleparallel geometry with zero curvature and torsion while non-zero nonmetricity behaves as the gravitational force. Adak and Sert [39] explored a gravity model that is characterized by nonmetricity, discovering that the horizon becomes singular in symmetric teleparallel gravity. Adak et al [40] formulated a symmetric teleparallel gravity model incorporating the Lagrangian in the non-metricity tensor, comprehensively analyzing the variations applicable to gravitational formulations. They derived a set of solutions encompassing Schwarzschild, Schwarzschild-de Sitter and Reissner-Nordstrom solutions for specific parametric values. The spherical symmetric configuration in $f(Q)$ gravity was investigated in [41]. Maurya et al [42] noted the significant impact of the nonmetricity parameter and decoupling constant on the stability of CSs in $f(Q)$ gravity. Adak et al [43] delved into the broader realm of teleparallel geometry using differential forms. Their exploration encompassed the examination of specific instances such as metric and symmetric teleparallelism. They provided insights into the connections between formulations employing gauge fixings and those without gauge fixing. Additionally, the researchers introduced a technique for transforming Riemannian geometries into teleparallel structures.

Cosmological observations revealed that the universe is originated through a significant expansion of matter and energy. Scientists raise sparking numerous inquiries among the formation, evolution and structure of the universe. Delving into the enigmatic features of the universe cosmologists have focused on the roles played by galaxies, planets, clusters and stars. Cosmology also elucidates fundamental processes such as the evolution and ultimate fate of stars. In maintaining its equilibrium, star relay on the delicate balance between inward gravitational force and outward matter pressure. This equilibrium becomes precarious when pressure is insufficient to counterbalance the gravity, resulting in collapse of the star. This collapse gives rise to new compact objects with reduced radii known as compact remnants. Many researchers have been intrigued by the nature and precise composition of compact stars (CSs).

Among these celestial bodies, neutron stars have garnered significant in-

terest due to their captivating properties and structures. Baade and Zwicky [44] delved into the geometry of CSs attributing their formation to supernovae and confirming their existence with the discovery of pulsars [45]. The presence of neutron stars becomes valid by identification of pulsars which captivate the researchers to analysis its various attributes. Dev and Gleiser [46] explored physical attributes of rotating neutron stars. Mak and Harko [47] scrutinized the physical characteristics of pulsars assessing their stability based on sound speed method. Kalam et al [48] examined viable and stable CSs using Krori-Barua solutions. Rahaman et al [49] investigated the physical characteristics of CSs by employing EoS parameters. Maurya et al [50] explore viable characteristics of anisotropic stars by considering different metric elements. Singh and Pant [51] applied a similar technique to ascertain the interior geometry of CSs. Bhar et al [52] assessed viable and stable CSs. Jasim et al [53] delve a non-singular spherical symmetric for anisotropic weird stars using the Tolman-Kuchowicz solution.

Isotropy (equal principal stresses) is a common assumption in the study of self-gravitating systems, whenever the fluid approximation is used to describe the matter distribution of the object. This character of fluids is supported by a large amount of observational evidence, pointing towards the equality of principal stresses under a variety of circumstances. However, strong theoretical evidences presented in the last decades suggest that for certain density ranges, different kinds of physical phenomena may take place, giving rise to anisotropy. The number of physical processes giving rise to deviations from isotropy is quite large in both high and low density regimes. Thus, for highly dense systems, exotic phase transitions may occur during the process of gravitational collapse. The consideration of anisotropic fluids in the context of CSs is essential to accurate capture the complex physical phenomena that govern their structure and stability. The inclusion of anisotropic pressure allows for a more realistic representation of matter under extreme conditions, leading to improved theoretical models that align better with observational data and predictions regarding stellar evolution, gravitational collapse and oscillation modes. In the extreme gravitational environments of CSs, the pressure and density may not be uniform throughout the star.

Anisotropic fluids account for the directional dependence of pressure, which can arise from several factors such as nuclear interactions, rotation and magnetic fields. At high densities, the interactions between particles can create different pressures in different directions due to the influence of strong nuclear forces. Rapid rotation and strong magnetic fields can in-

duce anisotropic pressure distributions. For instance, a rotating star may experience greater pressure along its equatorial plane compared to its poles. Anisotropic models allow for a more flexible and realistic equation of state that can better describe the thermodynamic properties of the matter in these stars. In dense astrophysical environments, matter may undergo phase transitions (e.g., from hadronic matter to quark-gluon plasma), leading to anisotropic pressure components. Anisotropic fluids can lead to different stability conditions compared to isotropic ones. In CS models, stability against gravitational collapse and oscillation modes can be better understood with anisotropic pressures, which might stabilize certain configurations that would be unstable in isotropic models. Anisotropic pressure can play a crucial role in avoiding singularities within the star, allowing for solutions that are physically viable. The detection of gravitational waves from neutron star mergers has revealed complex dynamics that can be modeled more accurately with anisotropic fluid dynamics, reflecting the actual physical processes at play. Anisotropic models can provide a richer structure for the field equations, enabling solutions that capture the complex nature of CSs. The influence of anisotropy has been extensively studied in [54]-[68].

In the study of CSs, the assumption of isotropic pressure might be convenient for simplification, but it often fails to capture the complex dynamics present in these objects. The physical processes inherent in stellar evolution, including dissipative phenomena and dynamic equilibrium, inherently lead to the development of pressure anisotropy, reinforcing the necessity to consider it in our models. Incorporating pressure anisotropy into the modeling of CSs is not merely an academic exercise, but it reflects the underlying physical realities of stellar dynamics. The inherent dissipative processes during stellar evolution guarantee that anisotropic pressures will manifest, shaping the final equilibrium state. Thus, models that overlook this essential feature risk failing to accurately describe the behavior of these fascinating astrophysical objects. Herrera [69] highlighted an important aspect that the pressure anisotropy is not merely a consequence of specific physical conditions in compact objects, but is rather an unavoidable outcome of the stellar evolution process. The consideration of anisotropic fluids in our model not only aligns with the physical phenomena expected in compact objects but also accommodates the natural evolution of pressure anisotropy during the system history. By adopting anisotropic fluid models, researchers can better capture the essential characteristics of CSs, leading to more accurate predictions of their behavior such as mass-radius relationships and stability criteria.

In astrophysics, CSs are objects that possess incredibly high densities and are supported by the balance between gravity and pressure due to their matter composition. To describe the internal structure and gravitational properties of such stars, it is crucial to find suitable solutions to the Einstein field equations that account for the behavior of matter under extreme gravitational and pressure conditions. One such solution is the Tolman-Kuchowicz spacetime. The Tolman-Kuchowicz spacetime is a specific solution to the field equations that has been applied to model the interior structure of CSs, such as neutron stars. The motivation for using this spacetime lies in capturing the essential physical properties of dense stellar objects and providing a framework for studying the behavior of matter and spacetime in extreme conditions. The Tolman-Kuchowicz spacetime is designed to satisfy several physical conditions necessary for realistic stellar models, i.e., regularity at the center. The metric components are regular at the center of the star, avoiding singularities and providing a smooth geometry. The solution can describe matter distributions with decreasing density and pressure from the center to the surface, mimicking the expected physical behavior of CS interiors. Thus, the Tolman-Kuchowicz spacetime is physically motivated in the context of CSs as it provides an exact solution to the field equations that satisfies the necessary physical conditions required for realistic models of CSs. It allows astrophysicists to explore how extreme densities and pressures in these stars influence their overall stability, making it a valuable tool for understanding the nature of compact objects.

The gravitational decoupling via complete geometric deformation method that has been introduced to explore the nonmetricity effects in relativistic astrophysics in [70]. Lohakare et al [71] studied simulates strange stars in $f(\mathcal{Q})$ gravity with an additional source under an electric field using gravitational decoupling technique. Maurya et al [72] examined compact objects in the framework of gravity by employing the method of gravitational decoupling. Kaur et al [73] presented a study on a spherically symmetric anisotropic solution in $f(\mathcal{Q})$ gravity in the framework of vanishing complexity formalism. Maurya et al [74] attempted to find an anisotropic solution for a CS generated by gravitational decoupling in $f(\mathcal{Q})$ gravity theory having a null complexity factor. Maurya et al [75] investigated the effect of $f(\mathcal{Q})$ parameters on two classes of exact spherically symmetric self-bound isotropic solutions for compact objects. Kumar et al [76] investigated the physical behavior and stability of charged CSs in $f(\mathcal{Q})$ gravity. Errehymy [77] et al presented a rigorous study of compact objects beyond the standard limit in $f(\mathcal{Q})$ gravity in

particular $f(\mathcal{Q}) = b_1 \mathcal{Q} + b_2$, where b_1 and b_2 are constants. Chaudhary et al [78] examined the properties of wormhole solutions in the this modified context. They analyzed that their findings contribute to the current discussion about alternative gravity theories and exotic spacetime geometries. Maurya et al [79] achieved a significant leap forward in understanding compact stellar systems and the modified $f(\mathcal{Q})$ gravity theory. Their investigation advances our knowledge of compact stellar systems and supports the evolution of the modified $f(\mathcal{Q})$ theory of gravity, opening the way for more breakthroughs in this field. Maurya et al [80] explored the possibility of existing a novel class of compact charged spheres based on a charged perfect fluid in the realm of $f(\mathcal{Q})$ theory. Mustafa et al [81] predicted the mass-radius relation along with the maximum mass limit of several objects for different parameter values by assuming two different surface densities and discovered that the compactness rises when density increases. We have also discussed the compact objects in different modified theories of gravity [82]-[84].

Jasim et al [85] analyzed a singularity-free model for the spherically symmetric anisotropic strange stars under Einstein general theory of relativity by exploiting the Tolman-Kuchowicz metric. Biswas et al [86] proposed a relativistic model of a static spherically symmetric anisotropic strange star with the help of Tolman-Kuchowicz metric potentials. Shamir and Fayyaz [87] presented the Einstein-Maxwell equations which are described by the spherically symmetric spacetime in the presence of charge by exploiting the Tolman-Kuchowicz spacetime. Shamir and Naz [88] explored some relativistic configurations of stellar objects for static spherically symmetric structures in the context of modified gravity by exploiting the Tolman-Kuchowicz spacetime. Raj et [89] studied the geometry of SAX J 1808.4-3658 CS with charged matter configuration in the framework of modified gravity theory using the metric potentials proposed by Tolman-Kuchowicz. Ditta and Xia [90] explored the stellar structures by employing Karmarkar condition Tolman-Kuchowicz metric components with the anisotropic source of the matter distribution in the background of Rastall teleparallel gravity. Bandyopadhyay and Biswas [91] studied the mass-radius relation of the specific CS in the background of the late time accelerated Universe and to achieve the equation of state of the core matter under stable equilibrium in modified gravity using Tolman-Kuchowicz metric potentials.

Singh et al [92] examine the physical behavior of CSs through karmarkar condition in $f(\mathcal{R}, T)$ theory. The use of karmarkar condition to investigate the viable behavior of strange stars in $f(\mathcal{R}, T)$ theory has been studied

in [93]. Biswas et al [94] proposed a realistic model for a static spherically symmetric anisotropic weird star using Tolman-Kuchowicz metric potentials. Shamir and Naz [95] utilized the Tolman-Kuchowicz spacetime to investigate configurations of static spherically symmetric structures under altered theory. In Brans-Dicke theory, Majid and Sharif [96] developed anisotropic model for weird star by deriving field equations for the Tolman-Kuchowicz ansatz. Javed et al [97] examined anisotropic sphere star and derived equations of motion for anisotropic matter distribution. Maurya et al [98] explored anisotropic matter distributions of CSs in the curvature-matter coupled theory.

This paper is structured in following pattern. Section 2 derives the equations of motion using the Tolman-Kuchowicz solution. This section also manipulates the unknown parameters through matching conditions. In Section 3, we evaluate the physical behavior of the CSs. In Section 4 stability of considered CSs is influenced through the sound speed and adiabatic index. Finally, we present a summary of our findings and implications in section 5.

2 Extended Symmetric Teleparallel Theory

The corresponding action is expressed as [99]

$$S = \int \left(\frac{1}{2} f(\mathcal{Q}) + L_m \right) \sqrt{-g} d^4x. \quad (1)$$

The non-metricity and deformation tensor are defined as

$$\begin{aligned} \mathcal{Q} &\equiv -g^{\varphi\psi} (L^{\varrho}_{\iota\varphi} L^{\iota}_{\varrho\psi} - L^{\varrho}_{\iota\varrho} L^{\iota}_{\varphi\psi}), \\ L^{\varrho}_{\iota\varphi} &\equiv -\frac{1}{2} g^{\varrho\varepsilon} (\nabla_{\varphi} g_{\iota\varepsilon} + \nabla_{\iota} g_{\varepsilon\varrho} - \nabla_{\varepsilon} g_{\iota\varphi}). \end{aligned} \quad (2)$$

The superpotential in terms of non-metricity is given by

$$P^{\varrho}_{\varphi\psi} = -\frac{1}{2} L^{\varrho}_{\varphi\psi} + \frac{1}{4} (\mathcal{Q}^{\varrho} - \bar{\mathcal{Q}}^{\varrho}) g_{\varphi\psi} - \frac{1}{4} \delta^{\varrho}_{(\varphi} \mathcal{Q}_{\psi)}. \quad (3)$$

The relation for \mathcal{Q} using superpotential is expressed as

$$\mathcal{Q} = -\mathcal{Q}_{\varrho\varphi\psi} P^{\varrho\varphi\psi} = -\frac{1}{4} (-\mathcal{Q}^{\varrho\psi\iota} \mathcal{Q}_{\varrho\psi\iota} + 2\mathcal{Q}^{\varrho\psi\iota} \mathcal{Q}_{\iota\varrho\psi} - 2\mathcal{Q}^{\iota} \bar{\mathcal{Q}}_{\iota} + \mathcal{Q}^{\iota} \mathcal{Q}_{\iota}). \quad (4)$$

The resulting field equations are

$$\frac{2}{\sqrt{-g}}\nabla_{\varrho}(\sqrt{-g}f_{\mathcal{Q}}P_{\varphi\psi}^{\varrho}) + \frac{1}{2}g_{\varphi\psi}f + f_{\mathcal{Q}}(P_{\varphi\varrho\epsilon}\mathcal{Q}_{\psi}{}^{\varrho\epsilon} - 2\mathcal{Q}_{\varrho\epsilon\varphi}P^{\varrho\epsilon}{}_{\psi}) = -T_{\varphi\psi}, \quad (5)$$

where $f \equiv f(\mathcal{Q})$ and $f_{\mathcal{Q}} = \frac{\partial f}{\partial \mathcal{Q}}$. The solution to these modified field equations may provide valuable understanding of gravity's behavior in this framework.

We analyze the compact stellar structures by studying static spherical spacetime as

$$ds^2 = -dt^2 e^{\nu(r)} + dr^2 e^{\lambda(r)} + d\theta^2 r^2 + d\phi^2 r^2 \sin^2 \theta, \quad (6)$$

where $e^{\nu(r)}$ and $e^{\lambda(r)}$ are metric potentials which ensures that the spacetime is static. We consider the anisotropic matter distribution as

$$T_{\varphi\psi} = \rho u_{\varphi} u_{\psi} + (u_{\varphi} u_{\psi} + g_{\varphi\psi})P_t + (P_r - P_t)v_{\varphi} v_{\psi}, \quad (7)$$

where u_{φ} and v_{ψ} represent four-velocity and four-vector of the fluid, respectively. Using Eq.(6), we have

$$\mathcal{Q} = -\frac{2}{r^2 e^{\lambda}}(1 + r\nu'), \quad (8)$$

where prime represents the radial coordinate derivative. The resulting field equations are given as follows

$$\rho = \frac{f}{2} - f_{\mathcal{Q}}\left(\mathcal{Q} + \frac{1}{r^2} + \frac{e^{-\lambda}}{r}(\nu' + \lambda')\right), \quad (9)$$

$$P_r = f_{\mathcal{Q}}\left(\mathcal{Q} + \frac{1}{r^2}\right) - \frac{f}{2}, \quad (10)$$

$$P_t = f_{\mathcal{Q}}\left(\frac{\mathcal{Q}}{2} - e^{-\lambda}\frac{\nu''}{2} + \left(\frac{\nu'}{4} + \frac{1}{2r}\right) \times (\nu' - \lambda')\right) - \frac{f}{2}, \quad (11)$$

$$0 = \frac{\cot \theta}{2}\mathcal{Q}'f_{\mathcal{Q}\mathcal{Q}}. \quad (12)$$

In the context of the $f(\mathcal{T})$ theory, the functional form of $f(\mathcal{T})$ is restricted by the non-zero off-diagonal metric components of the field equations [100], which arise from a particular gauge choice. This limitation also affects the functional form of $f(\mathcal{Q})$ theory, which is the mathematical foundation for constructing models based on $f(\mathcal{Q})$ gravity. In light of the discussion above,

we only consider $f_{\mathcal{Q}\mathcal{Q}} \neq 0$ in Eq. (12) to obtain the solution of $f(\mathcal{Q})$ gravity and its corresponding functional form becomes

$$f_{\mathcal{Q}\mathcal{Q}} = 0 \Rightarrow f_{\mathcal{Q}} = M_1 \Rightarrow f = M_1 \mathcal{Q} + M_2, \quad (13)$$

where M_1 and M_2 are integration constants. Using Eq.(12), we obtain the field equations as

$$\rho = \frac{1}{2r^2}(2M_1 + 2e^{-\lambda}M_1(r\lambda' - 1) - r^2M_2), \quad (14)$$

$$P_r = \frac{1}{r^2}(-2M_1 + 2e^{-\lambda}M_1(r\nu' + 1) + r^2M_2), \quad (15)$$

$$P_t = \frac{e^{-\lambda}}{4r}(2e^{\lambda}rM_2 + M_1(2 + r\nu')(\nu' - \lambda') + 2rM_1\nu''). \quad (16)$$

2.1 Matching Conditions

The fundamental boundary metric remains unchanged, whether it is generated from the internal and external geometry of the star. This approach assures that the metric parts will remain continuous over the boundary surface, irrespective of the coordinate system. The Jebsen-Birkhoff theorem states that all spherically symmetric vacuum solutions of field equations have to be asymptotically flat and static. The Schwarzschild solution is considered as the best option for the exterior geometry to investigate the CSs. The Schwarzschild solution can be accommodate for selection for the appropriate feasible $f(\mathcal{Q})$ gravity model with non-zero density and pressure. Although, this aspect might cause to violate Birkhoff theorem [101] in modified theories of gravity. Many researchers have contributed an immense amount of work on matching criteria. Goswami et al [105] showed that the junction conditions that arise in the expanded theories of gravity impose some limitations on the star objects. For this purpose, many researches [106]-[109] have considered the Schwarzschild solution, giving some intriguing outcomes. We consider exterior region as

$$ds^2 = -dt^2\aleph + dr^2\aleph^{-1} + d\theta^2r^2 + d\phi^2r^2\sin^2\theta, \quad (17)$$

where $\aleph = 1 - \frac{2M}{r}$. The gravitational collapse of massive stars generates fascinating objects known as CSs. It is essential to comprehend their composition, structure and behavior, to improve our understanding about astrophysics and basic physics. In order to describe the various aspects and

features such as density profiles, temperature and pressure, we consider the Tolman-Kuchowicz solutions with arbitrary constants (α, β, B, C) as

$$e^\nu = e^{Br^2 + 2\ln C}, \quad e^\lambda = 1 + \alpha r^2 + \beta r^4. \quad (18)$$

The unknown constants can be found using the Darmois junction conditions. By imposing these conditions, researchers can model the behavior of matter in celestial objects, leading to a deeper understanding of their physical properties. First Darmois junction condition governs the matching of solutions across the boundary of two spacetimes. This condition ensures the continuity of the metric tensor and its first derivative across the boundary between two regions of spacetime, where each region can have its own metric describing the curvature of spacetime. This junction condition is used to connect two different solutions of field equations, which describe the gravitational field of a given distribution of matter and energy. This condition is necessary when there is a boundary, such as a surface or a hypersurface, between two regions of spacetime that have different physical properties. This involves matching the components of the metric tensor and its derivatives at the boundary, making sure that the gravitational field remains smooth and continuous across that boundary. By satisfying this condition, one can create a consistent and continuous spacetime geometry that smoothly transitions from one solution to another. This conditions is particularly relevant in scenarios involving compact objects like black holes or stars, where the gravitational field transitions from being described by the exterior solution (e.g., Schwarzschild metric) to an interior solution (e.g., a solution describing the matter distribution in the object). This is crucial for constructing physically meaningful spacetimes in such cases. The second fundamental (continuity of extrinsic curvature at the hypersurface) gives that radial pressure is zero at the boundary. Hence, Darmois junction conditions are the mathematical requirements that enable a coherent description of the gravitational field in these situations. The continuations of the first and second fundamental forms at the surface boundary ($r = R$) gives

$$\begin{aligned} \alpha &= \frac{1}{R(R-2M)} + \frac{MR}{2(R-2M)^4} - \frac{1}{R^2}, \\ \beta &= \frac{-M}{2R(R-2M)^4} \\ B &= \frac{M}{R^2(R-2M)}, \end{aligned}$$

Table 1: Approximated Values of unknown constants.

Star Models	M(km)	R(km)	$\alpha(km^{-2})$	$\beta(km^{-2})$	$B(km^{-2})$	$C(km^{-2})$
Cen X-3 [110]	1.49 ± 0.08	9.178 ± 0.13	0.0222	-0.0002	0.0030	0.7260
EXO 1785-248 [111]	1.30 ± 0.2	10.10 ± 0.44	0.0314	-0.0003	0.0039	0.7284
LMC X-4 [110]	1.04 ± 0.09	8.301 ± 0.2	0.0117	-0.0006	0.0069	0.7302

$$C = e^{\sqrt{\ln(1-\frac{2M}{R})-\frac{M}{R-2M}}},$$

$$P_r(r=R) = 0.$$

Now, using Tolman-Kuchowicz spacetime constraints resulting field equations are

$$\rho = \frac{-1}{2r^2} \left[2\alpha r^2 + 6br^4 + r^2 - 4 \right], \quad (19)$$

$$P_r = \frac{-1}{r^2} \left[4 + 4Br^2 + 2\alpha Br^4 + 2\alpha r^2 + 4B\beta + 2\beta r^4 - r^2 \right], \quad (20)$$

$$P_t = \frac{-(1 + \alpha r^2 + \beta r^4)}{4r} \left[2r(1 + \alpha r^2 + \beta r^4) + (2 + 2Br^2) \right. \\ \left. \times (2Br + 2\alpha Br^3 + 2B\beta r^5 - 2\alpha r)(1 + \alpha r^2 + \beta r^4)^{-1} + 4rB \right]. \quad (21)$$

We consider three CSs models Cen X-3, EXO 1785-248 and LMC X-4. We used green color for Cen X-3, red color for EXO 1785-248 and blue color for LMC X-4 for all graphs respectively. The values of mass, radius and constants for the proposed CSs are given in Table 1. In the analysis of stellar objects, it is essential to examine the behavior of metric elements to ascertain the smoothness and absence of singularities in the spacetime. The graphical representation depicted in Figure 1 serves as a crucial tool in this evaluation process. It is clear that both metric components display consistent patterns and show an increasing trend. This behavior is significant as it indicates the absence of any abrupt or irregular fluctuations in the spacetime metrics associated with the stellar objects under consideration. Thus, based on the graphical analysis presented in Figure 1, we can assert that the spacetime appears to be smooth and devoid of singularities, meeting the required criteria for our investigation.

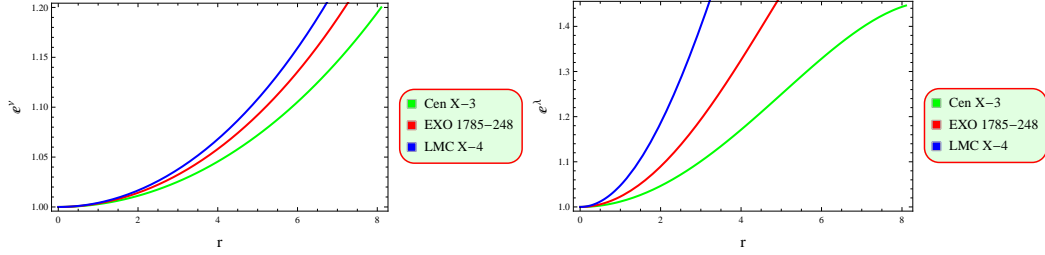


Figure 1: Graphical evaluation of metric potentials corresponding to radial coordinate for $M_1 = -0.1$ and $M_2 = 10$.

3 Physical Characteristics

This section delves into an exploration of the physical characteristics exhibited by anisotropic CSs, accompanied by graphical visualizations to examine their characteristics. Our findings with observational data has the potential to provide compelling support for the proposed model. Our analysis encompasses various realistic aspects of compact objects by graphical representations.

3.1 Behavior of Matter Contents

The interior of stars is characterized by an exceptionally dense profile, leading to the maximum concentration of effective matter contents. In Figures 2 and 3, we present the behavior of matter contents and their derivatives for considered CSs. These figures reveal a positive decrease in the physical parameters and vanishing points at the boundary, indicating dense profile of stars. The radial derivative of matter contents exhibit a consistent pattern, affirming the existence of dense CSs in the $f(Q)$ framework.

Pressure anisotropy ($\Delta = P_t - P_r$) refers to the phenomenon where pressure in a system is not uniform in all directions. In other words, the pressure can vary depending on the direction in which it is measured. Positive anisotropy implies outward pressure, while negative anisotropy signifies inward pressure. Positive anisotropy refers to the situation where the tangential pressure P_t exceeds the radial pressure P_r at a given point inside the star, i.e., $P_t > P_r$. This difference in pressures generates an outward-directed anisotropic force. This anisotropic pressure can significantly influence the stability and structure of astrophysical objects, particularly in the modeling

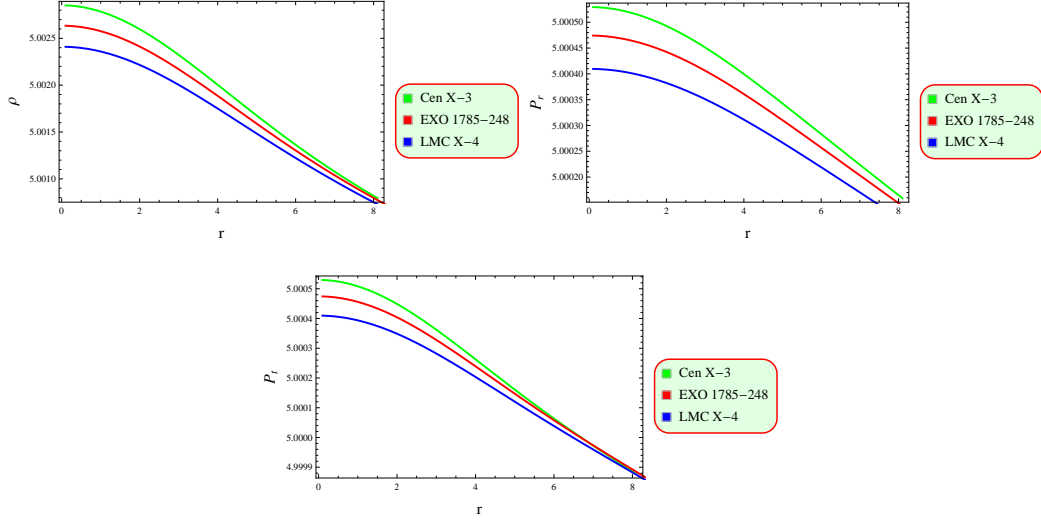


Figure 2: Graphs of energy density, radial pressure and tangential pressure corresponding to radial coordinate for $M_1 = -0.1$ and $M_2 = 10$ are maximum at the center of the stars and monotonically decreasing as the radial distance increases, revealing a highly compact profile of the proposed CSs.

of CSs like neutron stars. In the presence of strong gravitational forces, particularly near the core of the star, this outward-directed anisotropy offers an extra counterbalance to gravity. The outward pressure provided by the positive anisotropy allows the star to maintain equilibrium at higher densities, which can potentially lead to a larger maximum mass compared to isotropic stars. This is significant in explaining the existence of very massive neutron stars. Positive anisotropy can also result in more compact stellar configurations, where the star radius is smaller for a given mass. This compactness may alter the star surface gravity and its observable properties.

Figure 4 represents that this anisotropy illustrates an anti gravitational behavior essential for compact structures.

3.2 Energy Bounds

The energy conditions consist of inequalities that place constraints on the stress-energy tensor, governing the interaction between matter and energy in gravitational field. These constraints are crucial for assessing the feasibility of CSs, expressed as null ($9\rho + P_r \geq 0$, $\rho + P_t \geq 0$), dominant ($\rho \pm P_r \geq$

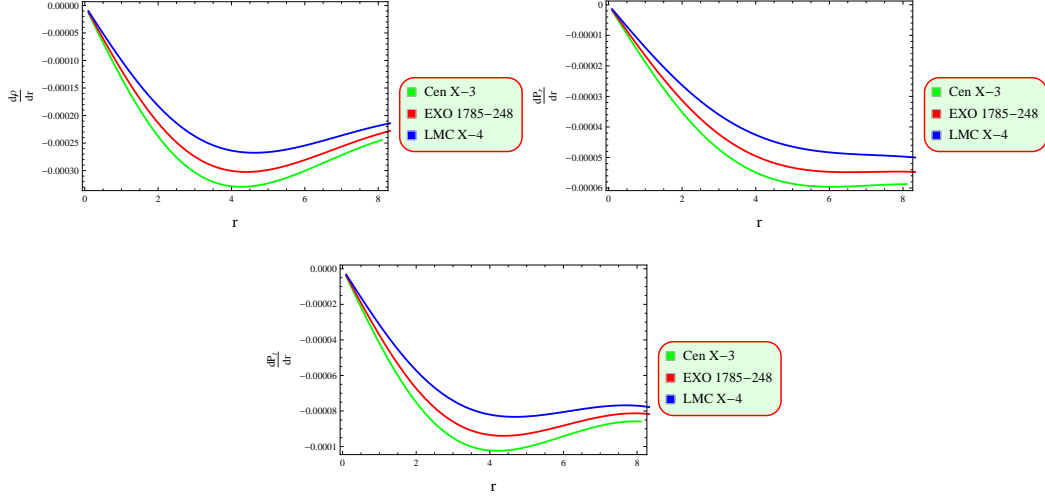


Figure 3: Plots of Gradients of energy density, radial pressure and tangential pressure corresponding to radial coordinate for $M_1 = -0.1$ and $M_2 = 10$ are zero at the center and become negative as one moves away from the core, which confirms the existence of highly compact configuration in $f(\mathcal{Q})$ theory.

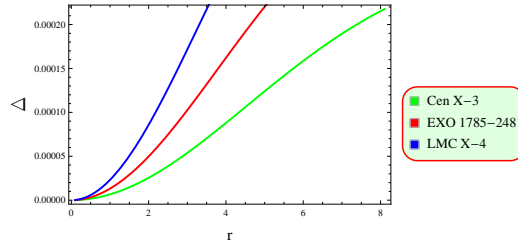


Figure 4: Behavior of anisotropy corresponding to radial coordinate is positively increasing for all CSs, which ensures the existence of repulsive force that is necessary for massive geometries.

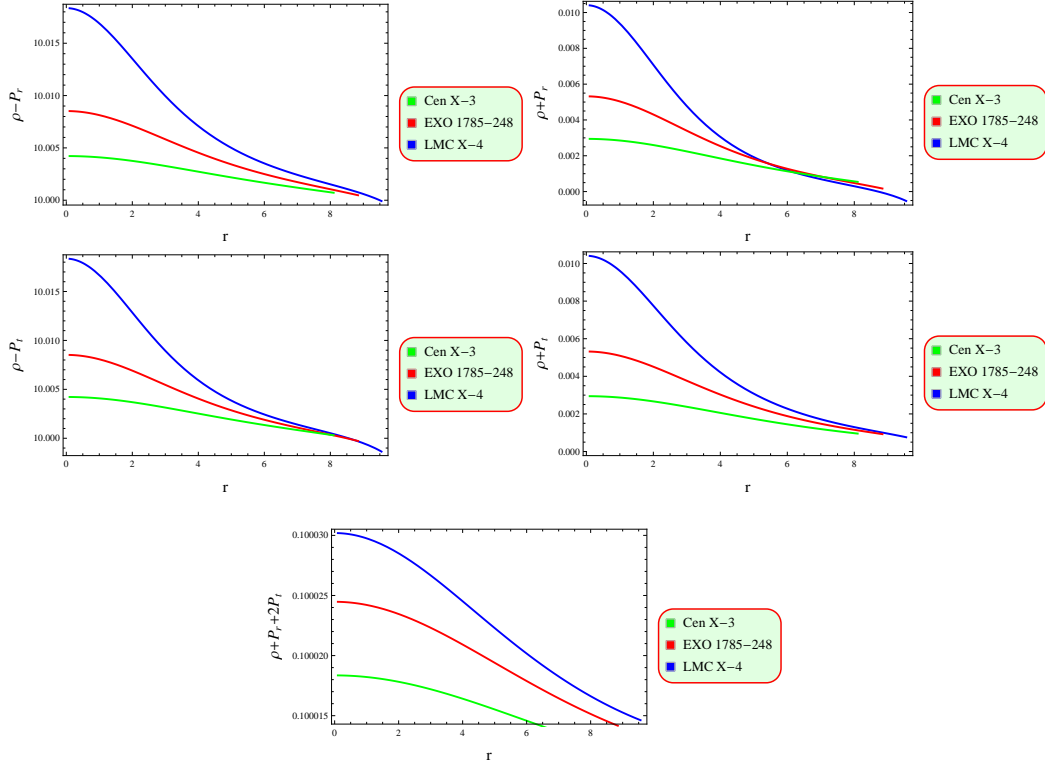


Figure 5: Plots of energy conditions corresponding to radial coordinate for $M_1 = -0.1$ and $M_2 = 10$ are positive which demonstrate that the proposed star candidates are physically viable due to the existence of normal matter inside the stars.

$0, \rho \pm P_t \geq 0$), weak ($\rho + P_r \geq 0, \rho + P_t \geq 0, \rho \geq 0$) and strong $\rho + P_r \geq 0, \rho + P_t \geq 0, \rho + P_r + 2P_t \geq 0$ energy conditions. In Figure 5, it is demonstrated that the considered star candidates maintain physical viability because they meet all energy constraints in the presence of $f(\mathcal{Q})$ terms, which affirms the presence of ordinary matter inside the stars.

3.3 Analysis of Different Physical Aspects

The mass of anisotropic stars is defined as

$$M(r) = \int_0^r \pi r^2 \rho dr \quad (22)$$

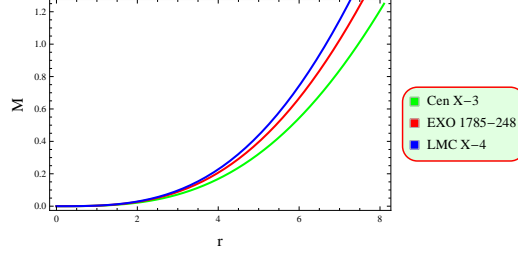


Figure 6: Behavior of mass function corresponding to radial coordinate manifests that the mass increases positively and monotonically as the radius increases. Also, $M \rightarrow 0$ as $r \rightarrow 0$ which shows that the mass function is regular at the center of CSs.

In Figure 6, the mass function exhibits regularity at the core of stars under consideration showing a monotonic increase with radius. This observation indicates the absence of singularities or irregularities in the mass distribution at the center of these celestial bodies. To gain insights into the structural composition of these objects, various physical aspects can be explored. One crucial parameter for analyzing CSs is the compactness function, denoted as ($u = \frac{M}{r}$). Buchdahl [112] established a specific condition for viable CSs, requiring the compactness factor to satisfy $u < \frac{4}{9}$. This criterion is essential for understanding the stability of stars.

Another important factor is surface redshift, which measures the alteration in the wavelength of light emitted from the star surface as a result of intense gravitational effects. This parameter provides valuable insight the characteristics of the stars. The redshift in terms of compactness can be formulated as

$$Z_s + 1 = \sqrt{1 - 2\mu(r)} \quad (23)$$

Figure 7 shows that surface redshift satisfied the required limit.

3.4 State Parameter

The equation of state (EoS) parameter plays a crucial role in understanding the physical properties and internal structure of CSs. It provides a relationship between the pressure and the energy density of the matter inside the star, defined as $P = \omega\rho$, where ω is the equation of state parameter. The EoS parameter captures the behavior of nuclear matter, including interactions between neutrons, protons and possibly hyperons or other exotic

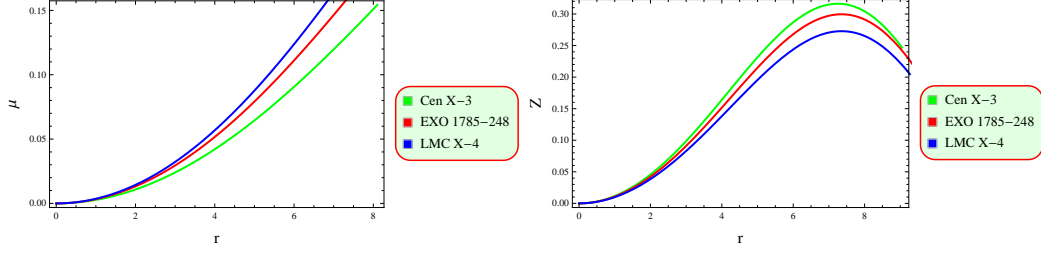


Figure 7: Behavior of compactness and redshift functions corresponding to radial coordinate lie in the specified limits ($u < 4/9$ and $Z_s < 5.211$).

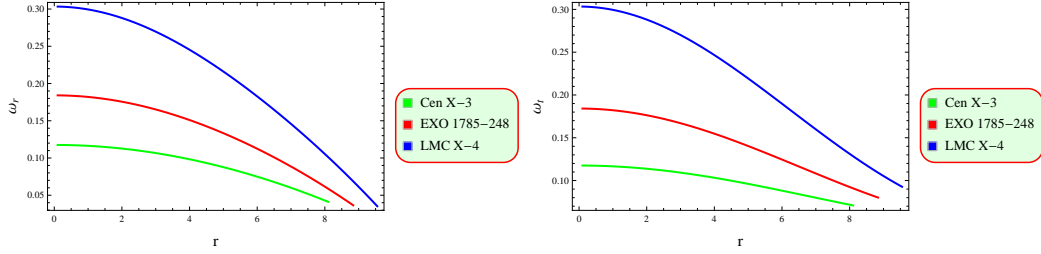


Figure 8: Plot of radial and tangential EoS parameters corresponding to radial coordinate for $M_1 = -0.1$ and $M_2 = 10$.

particles. As the density increases towards the star's center, different phases of matter might emerge and the EoS parameter must reflect these changes. Thus, the EoS parameter serves as a bridge between microphysical interactions inside CSs and their macroscopic observables, providing crucial insights into the nature of ultra-dense matter and the ultimate fate of massive stars. For anisotropic CSs, the radial and transversal forms of the EoS parameters ($\omega_r = \frac{P_r}{\rho}, \omega_t = \frac{P_t}{\rho}$) must lie in $[0,1]$ for the effectiveness of considered star candidates. The corresponding parameters are described as

$$\begin{aligned} \omega_r &= \frac{-1}{r^2} \left[4 + 4Br^2 + 2\alpha Br^4 + 2\alpha r^2 + 4B\beta + 2\beta r^4 - r^2 \right] \\ &\times \left[\frac{1}{2r^2} \{ 4 - 2\alpha r^2 - 6\beta r^4 - r^2 \} \right]^{-1}, \\ \omega_t &= \left[\frac{-(1 + \alpha r^2 + \beta r^4)}{4r} \{ 2r(1 + \alpha r^2 + \beta r^4) \} \right] \end{aligned}$$

$$\begin{aligned}
& + (2 + 2Br^2) \left(\frac{2Br + 2\alpha Br^3 + 2B\beta r^5 - 2\alpha r}{1 + \alpha r^2 + \beta r^4} \right) + 4rB \Bigg] \\
& \times \left[\frac{1}{2r^2} \{4 - 2\alpha r^2 - 6br^4 - r^2\} \right]^{-1}.
\end{aligned}$$

Figure 8 shows that our proposed stars are viable as the state parameters remain in their specified limits.

4 Stability Analysis

Stability analysis delves into the repercussions of minor disturbances on the integrity of stellar objects, investigating whether they would revert to their initial state of equilibrium or undergo substantial transformations. It holds significant importance in gaining insights into the credibility and coherence of cosmic structures. The examination of conditions ensuring the stability of these structures against diverse oscillation modes is a key aspect of stability analysis. The stability is influenced by both the geometry of these structures and the characteristics of the matter constituting. Various methods are employed in this context to analysis the stability of CSs.

4.1 Tolman-oppenheimer-Volkoff

This equation provides insight into how different forces acting on a system maintain its stability. It sheds light on the delicate balance between a star's internal pressure and the gravitational force. This equation play pivotal role in gaining insights in internal composition and characteristics of stars. Now, by using field equations Eqs.(14)-Eqs.(16), we have TOV equation in the context of $f(Q)$ theory as follows

$$\frac{2\Delta}{r} - \frac{\nu'(\rho + P_r)}{2} - (P_r)' = 0. \quad (24)$$

This equation gives the information on the cosmic balance resulting from the various forces, i.e., anisotropic (F_a), hydrostatic (F_h) and gravitational (F_g). These forces in this modified framework turns out to be

$$F_g = -\frac{B}{2r} \left[(4 - 2\alpha r^2 - 6br^4 - r^2) \right] + \frac{1}{r^2} \left[(4Br^2 e^{-Ar^2} + 2e^{-Ar^2} + r^2 - 2) \right],$$

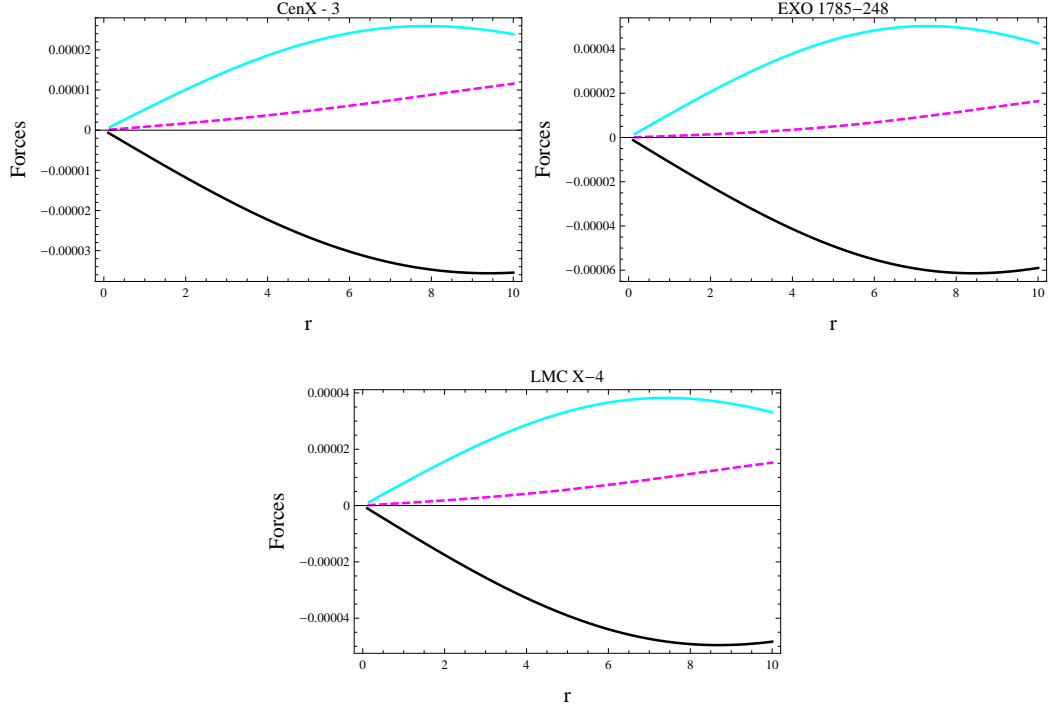


Figure 9: Plot of TOV equation corresponding to radial coordinate for $M_1 = -0.1$ and $M_2 = 10$.

$$\begin{aligned}
F_h &= \left[\left\{ \frac{-2}{r^5} (-4 - 4Br^2 - 2\alpha Br^4 - 2\alpha r^2 - 4B\beta - 2\beta r^4 + r^2) \right. \right. \\
&\quad \left. \left. + \frac{1}{r^2} (-8Br - 8\alpha Br^3 - 8\alpha r - 24B\beta r^5 - 8\beta r^3 + 2r) \right\} \right], \\
F_a &= -\frac{2}{r} \left[\frac{(1 + \alpha r^2 + \beta r^4)}{4r} \{ 2r(1 + \alpha r^2 + \beta r^4) \right. \\
&\quad \left. + (2 + 2Br^2) \left(\frac{2Br + 2\alpha Br^3 + 2B\beta r^5 - 2\alpha r}{1 + \alpha r^2 + \beta r^4} \right) + 4rB \right\} \\
&\quad \left. - \left\{ \frac{1}{r^2} (-4 - 4Br^2 - 2\alpha Br^4 - 2\alpha r^2 - 4B\beta - 2\beta r^4 + r^2) \right\} \right].
\end{aligned}$$

Figure 9 shows that the proposed star candidates are in equilibrium condition.

4.2 Casuality Condition

We examine the stability through casuality condition for the considered stars models. In causality condition, the tangential $\nu_{st} = \frac{dP_t}{d\rho}$ and radial $\nu_{sr} = \frac{dP_r}{d\rho}$ components should lie in interval $[0, 1]$ [113]. The components of sound speed are given by

$$\begin{aligned}
\nu_{sr} &= \left[\left\{ \frac{-2}{r^5}(-4 - 4Br^2 - 2\alpha Br^4 - 2\alpha r^2 - 4B\beta - 2\beta r^4 + r^2) \right. \right. \\
&\quad \left. \left. + \frac{1}{r^2}(-8Br - 8\alpha Br^3 - 8\alpha r - 24B\beta r^5 - 8\beta r^3 + 2r) \right\} \right] \\
&\quad \times \left[\left\{ \frac{-1}{r^3}(4 - 2\alpha r^2 - \beta r^4 - r^2) + \frac{1}{2r^2}(-4\alpha r - 24\beta r^3 - 2r) \right\} \right]^{-1}, \\
\nu_{st} &= \left[\frac{(-1 + \alpha r^3 + \beta r^5)}{4r} \{2r(1 + \alpha r^2 + \beta r^4) \right. \\
&\quad \left. + (2 + 2Br^2) \left(\frac{2Br + 2\alpha Br^3 + 2B\beta r^5 - 2\alpha r}{1 + \alpha r^2 + \beta r^4} \right) + 4rB \right\} \\
&\quad + \left[\left\{ \frac{(1 + \alpha r^2 + \beta r^4)}{4r} \right\} + \{2 + 4B + 6\alpha r^2 + 10\beta r^5 \right. \\
&\quad \left. + \frac{8B^2 r^2 + 8\alpha B^2 r^4 + 8B^2 \beta r^6 - 8\alpha B r^2}{1 + \alpha r^2 + \beta r^4} + (2 + 2Br^2) \right. \\
&\quad \left. \times \left(\frac{2B + 6\alpha B r^2}{1 + \alpha r^2 + \beta r^4} - \frac{(2Br + 2\alpha Br^3 + 2B\beta r^5 - 2\alpha r)(2\alpha r + 16\beta r^3)}{(1 + \alpha r^2 + \beta r^4)^2} \right) \right\} \\
&\quad \left. \times \left[\left\{ \frac{-1}{r^3}(4 - 2\alpha r^2 - \beta r^4 - r^2) + \frac{1}{2r^2}(-4\alpha r - 24\beta r^3 - 2r) \right\} \right]^{-1} \right]
\end{aligned}$$

Figure 10 determines that the considered stars are stable and lie in specified limits. Thus, considered stars are physically stable in $f(Q)$ theory.

4.3 Herrera Cracking Approach

The concept of cracking is associated to the tendency of a fluid distribution to “split”, once it abandons the equilibrium as consequence of perturbations. Thus, one can say that once the system has abandoned the equilibrium, there is a cracking, whenever its inner part tends to collapse whereas its outer part tends to expand. The cracking takes place at the surface separating the two regions. When the inner part tends to expand and the outer one tends to

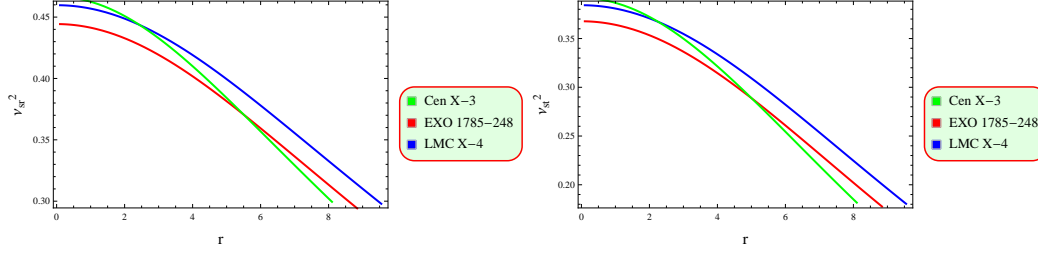


Figure 10: Graphs of radial sound speed component and tangential sound speed component corresponding to radial coordinate lie in $[0,1]$ in the presence of modified terms, which show that spherically symmetric solutions are in the stable state.

collapse we say that there is an overturning. It is worthwhile to mention that the concepts of stability and cracking are different, although they are often confused. The term stability refers to the capacity of a given fluid distribution to return to equilibrium once it has been removed from it. The fact that the speeds of sound are not superluminal does not assure in any way the stability of the object, it only ensures causality. The cracking only implies the tendency of the system to split immediately after leaving the equilibrium. Whatever happens next, whether the system enters into a dynamic regime, or returns to equilibrium, is independent of the concept of cracking. Of course the occurrence of cracking will affect the future of the fluid configuration in either case.

We use a Herrera cracking method for the stability of stars [114]. A crucial factor in identifying the stability regions is difference between sound speed in radial and transverse directions. The area is considered unstable if the inequality is not satisfied by this difference. In particular for stable regions, $0 \leq |\nu_{st} - \nu_{sr}| \leq 1$. The stars under consideration, satisfy these requirements as shown in Figure 11 which implies a stable state.

4.4 Adiabatic Index

Adiabatic index is another method which is used for the stability of CSs. The radial and tangential components are given as

$$\Gamma_r = \left(\frac{P_r + \rho}{P_r} \right) \nu_{sr}, \quad \Gamma_t = \left(\frac{P_t + \rho}{P_t} \right) \nu_{st}. \quad (25)$$

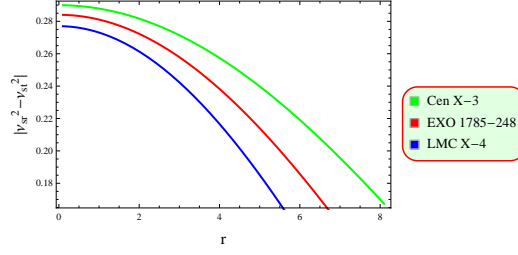


Figure 11: Graphs of Herrera cracking corresponding to radial coordinate determine that considered CSs are stable as they lie in the specified limit.

Using Eqs.(20)-Eqs.(22), we have

$$\begin{aligned}
\Gamma_r &= \left[\left\{ \frac{1}{2r^2}(4 - 2\alpha r^2 - 6br^4 - r^2) \right\} + \left\{ \frac{1}{r^2}(-4 - 4Br^2 - 2\alpha Br^4 - 2\alpha r^2 - 4B\beta - 2\beta r^4 + r^2) \right\} \right] \\
&\times \left[\frac{1}{r^2}(-4 - 4Br^2 - 2\alpha Br^4 - 2\alpha r^2 - 4B\beta - 2\beta r^4 + r^2) \right]^{-1} \\
&\times \left[\left\{ \frac{-2}{r^5}(-4 - 4Br^2 - 2\alpha Br^4 - 2\alpha r^2 - 4B\beta - 2\beta r^4 + r^2) \right. \right. \\
&+ \left. \left. \frac{1}{r^2}(-8Br - 8\alpha Br^3 - 8\alpha r - 24B\beta r^5 - 8\beta r^3 + 2r) \right\} \right] \\
&\times \left[\left\{ \frac{-1}{r^3}(4 - 2\alpha r^2 - \beta r^4 - r^2) + \frac{1}{2r^2}(-4\alpha r - 24\beta r^3 - 2r) \right\} \right]^{-1} \\
\Gamma_t &= \left[\left\{ \frac{1}{2r^2}(4 - 2\alpha r^2 - 6br^4 - r^2) \right\} + \left\{ \frac{-(1 + \alpha r^2 + \beta r^4)}{4r}(2r(1 + \alpha r^2 + \beta r^4)) \right. \right. \\
&+ \left. \left. (2 + 2Br^2)\left(\frac{2Br + 2\alpha Br^3 + 2B\beta r^5 - 2\alpha r}{1 + \alpha r^2 + \beta r^4}\right) + 4rB \right\} \right] \\
&\times \left[\frac{-(1 + \alpha r^2 + \beta r^4)}{4r} \{2r(1 + \alpha r^2 + \beta r^4)\} \right. \\
&+ \left. \left. (2 + 2Br^2)\left(\frac{2Br + 2\alpha Br^3 + 2B\beta r^5 - 2\alpha r}{1 + \alpha r^2 + \beta r^4}\right) + 4rB \right\} \right]^{-1} \\
&\times \left[\frac{(-1 + \alpha r^3 + \beta r^5)}{4r} \{2r(1 + \alpha r^2 + \beta r^4)\} \right.
\end{aligned}$$

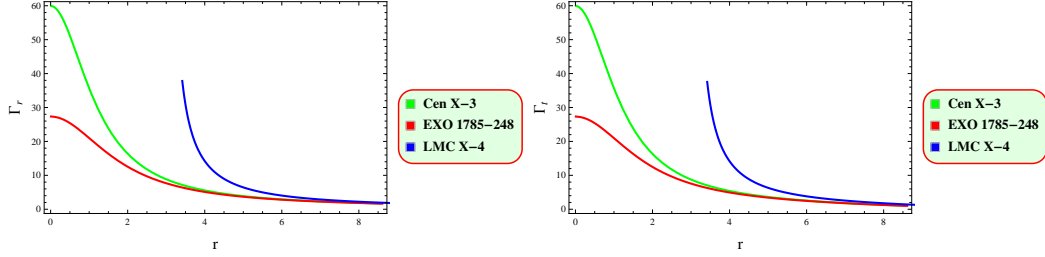


Figure 12: Plot of adiabatic index corresponding to radial coordinate for $M_1 = -0.1$ and $M_2 = 10$.

$$\begin{aligned}
& + (2 + 2Br^2) \left(\frac{2Br + 2\alpha Br^3 + 2B\beta r^5 - 2\alpha r}{1 + \alpha r^2 + \beta r^4} + 4rB \right) \Big] \\
& + \left[\left\{ \frac{(1 + \alpha r^2 + \beta r^4)}{4r} \right\} + \{2 + 4B + 6\alpha r^2 + 10\beta r^5\} \right. \\
& + \frac{8B^2 r^2 + 8\alpha B^2 r^4 + 8B^2 \beta r^6 - 8\alpha B r^2}{1 + \alpha r^2 + \beta r^4} + (2 + 2Br^2) \\
& \times \left(\frac{2B + 6\alpha Br^2}{1 + \alpha r^2 + \beta r^4} - \frac{(2Br + 2\alpha Br^3 + 2B\beta r^5 - 2\alpha r)(2\alpha r + 16\beta r^3)}{(1 + \alpha r^2 + \beta r^4)^2} \right) \Big] \\
& \times \left[\left\{ \frac{-1}{r^3} (4 - 2\alpha r^2 - \beta r^4 - r^2) + \frac{1}{2r^2} (-4\alpha r - 24\beta r^3 - 2r) \right\} \right]^{-1}
\end{aligned}$$

Chandrasekhar determine the condition that system is stable if $\Gamma > \frac{4}{3}$ otherwise unstable [115]. For all considered CSs, our system is stable as shown in Figure 12.

5 Conclusions

Modified gravity theories such as $f(\mathcal{Q})$ gravity have received considerable interest in recent years as alternate explanations to GR. This theory suggests alterations to the fundamental equations of gravity with the aim of addressing numerous unresolved inquiries in the fields of cosmology and astrophysics. A crucial method for assessing and limiting the validity of this modified gravity theory is by conducting astrophysical observations. This modified theory introduces extra independent variables that describe deviations from GR. This modified proposal aims to enhance our understanding of the principles that regulate the actions of matter and energy in the cosmos, providing

opportunities to investigate novel phenomena that may not be accounted for in GR. The inclusion of correction terms emphasize the significant results, imposing a large impact on the geometric feasibility. The $f(Q)$ theory is used as a mathematical tool to examine complex elements of gravitational dynamics on a large scale. The motivation behind the investigation of this theory involves analyzing its theoretical implications, its consistency with empirical facts and its importance in cosmological contexts.

In recent years, the discipline of theoretical physics has been greatly interested in studying CSs. These celestial entities provide considerable obstacles to our understanding of basic physics and offer distinct possibilities for studying extreme situations in the theoretical framework. Our study is centered around the investigation of anisotropic CSs in $f(Q)$ theory with the objective of exploring the enigmatic aspects of the cosmos. By examining anisotropic CSs in this theoretical framework, gravitational interactions unveil on both galactic and cosmic levels. This offers valuable understanding of how these components impact stellar structures. Studying these objects in this theory allows us to investigate the behavior of gravity under conditions of high curvature and density as gravity in CSs approaches its extreme limits. By examining the behavior of these compact celestial objects, we acquire significant knowledge about the properties of CSs.

This paper delves into the examination of the viability and stability of CSs utilizing the Tolman-Kuchowicz solution in the framework of $f(Q)$ theory. The values of unknown constants are given in Table 1. The specific model of this modified theory is developed to investigate the behavior of different physical quantities within the inner regions of stars. The key findings are summarized below.

- We have found that both metric elements (Figure 1) are consistent and fulfill the necessary conditions, i.e., they exhibit minimum value at the center of stars and then show monotonically increasing behavior.
- The behavior of fluid parameters (Figure 2) is positive and regular in the interior of CSs and diminish at the boundary. Also, the derivative of fluid parameters (Figure 3) is negative which presents a dense picture of the CSs.
- We have found that the anisotropic pressure (Figure 4) is directed outward which is necessary for compact stellar configuration

- All energy bounds are satisfied to confirm the presence of normal matter in the interior of CSs (Figure 5).
- We have found that the mass function is regular at the center of the star and show monotonically increasing behavior as the radial coordinate increases Figure 6. The compactness and redshift functions satisfy the required conditions Figure 7.
- The range of EoS parameters (Figure 8) lies between 0 and 1, which shows the viability of the considered model.
- The TOV equation shows that gravitational, hydrostatic, and anisotropic forces have a null impact for all proposed CSs (Figure). This suggests that the compact stellar models are in an equilibrium state.
- The stability limits, i.e., ν_{sr} and ν_{st} lies between 0 and 1 (causality condition), $0 < |\nu_t^2 - \nu_r^2| < 1$ (Herrera cracking) approach and $\Gamma > \frac{4}{3}$ (adiabatic index) are satisfied, which ensures the existence of physically stable CSs (Figures 10-12).

We have conducted an investigation into the viability and stability of CSs incorporating $f(\mathcal{Q})$ terms. Our analysis has unveiled a denser profile for CSs, demonstrated through a comprehensive examination of the derived solutions. In the context of $f(\mathcal{R}, \mathcal{T}^2)$ theory, it has been established that CSs are not physically feasible or stable at their center [?]. Our findings indicate that all the considered CSs exhibit both physical feasible as well as stability at their central position in $f(\mathcal{Q})$ theory. Therefore, our derived solutions provide stable formations of anisotropic CSs.

References

- [1] P.M. Garnavich, et al., *Astrophys. J.* **74**, 509 (1998).
- [2] A.G. Riess, et al., *Astron. J.* **116**, 1009 (1998).
- [3] A.G. Riess, et al., *Astron. J.* **607**, 665 (2004).
- [4] M. Tegmark, et al., *Phys. Rev. D* **69**, 103501 (2004).
- [5] D.N. Spergel, et al., *Astrophys. J. Suppl. Ser.* **148**, 175 (2003).

- [6] G. Cognola, et al.: Phys. Rev. D **77**, 046009 (2008).
- [7] A.D. Felice and S.R. Tsujikawa, Living Rev. Relativ. **13**, 161 (2010).
- [8] E.V. Linder, Phys. Rev. D **81**, 127301 (2010).
- [9] A. Jawad and A. Iqbal, Int. J. Mod. Phys. D **25**, 1650074 (2016).
- [10] A. Jawad, et al., Astrophys. Space Sci. **362**, 63(2017).
- [11] A. Jawad and S. Rani, Eur. Phys. J. C **76**, 704 (2016).
- [12] Debnath, U., Chattopadhyay, S., Hussain, I., Jamil, M. and Myrzakulov, R., Eur. Phys. J. C **72**(2024)1-6.
- [13] Sultana, S. and Chattopadhyay, S., Int. J. Geome. Meth. Mod. Phys., **21**(7)(2024)2450133-6396.
- [14] Saha, S., Chattopadhyay, S. and Gudekli, E., Eur. Phys. J. C **84**(3)(2024)314.
- [15] Chokyi, K.K. and Chattopadhyay, S., International Journal of Modern Physics D, **33**(2)(2024)2450002.
- [16] Saha, S., Chattopadhyay, S. and Gudekli, E., International Journal of Modern Physics D (2024)2450042.
- [17] M.Z. Gul, M. Sharif and I. Kanwal, New Astron. **109**, 102204 (2024).
- [18] H.S. Weyl, Preuss. Akad. Wiss. **1**, 465 (1918).
- [19] E. Cartan, Ann. Ec. Norm. **40**, 325 (1923).
- [20] R. Weitzenbock, *Invariantentheorie, noordhoff and groningen*, (1923).
- [21] J.B. Jimenez, et al., Phys. Rev. D **101**, 103507 (2020).
- [22] J. Lu, X. Zhao and G. Chee, Eur. Phys. J. C **79**, 530 (2019).
- [23] R. Lazkoz, et al., Phys. Rev. D **100**, 104027 (2019).
- [24] R.H. Lin and X.H. Zhai, Phys. Rev. D **103**, 124001 (2021).
- [25] F. D Ambrosio, et al., Phys. Rev. D **105**, 024042 (2022).

- [26] W. Wang, H. Chen and T. Katsuragawa, Phys. Rev. D **105**, 024060 (2022).
- [27] A. Delhom-Latorre, G.J. Olmo and M. Ronco, Phys. Lett. B **780**, 294 (2018).
- [28] K.F. Dialektopoulos, T.S. Koivisto and S. Capozziello, Eur. Phys. J. C **79**, 606 (2019).
- [29] B.J. Barros, et al., Dark Universe **30**, 100616 (2020).
- [30] F. Bajardi, D. Vernieri and S. Capozziello, Eur. Phys. J. Plus **135**, 912 (2020).
- [31] F. D Ambrosio, M. Garg and L. Heisenberg, Phys. Lett. B **811**, 135970 (2020).
- [32] I. Ayuso, R. Lazkoz and V. Salzano, Phys. Rev. D **103**, 063505 (2021).
- [33] K. Flathmann and M. Hohmann, Phys. Rev. D **103**, 044030 (2021).
- [34] N. Frusciante, Phys. Rev. D **103**, 044021 (2021).
- [35] W. Khylllep, A. Paliathanasis and J. Dutta, Phys. Rev. D **103**, 103521 (2021).
- [36] S. Capozziello and R. D Agostino, Phys. Lett. B **832**, 137229 (2022).
- [37] M. Adak, Turk. J. Phys. **30**, 379 (2006).
- [38] J.M. Nester and H.J. Yo, Chin. J. Phys. **37**, 113 (1999).
- [39] M. Adak and O. Sert, Turk. J. Phys. **29**, 1 (2005).
- [40] M. Adak, M. Kalay and O. Sert, Int. J. Mod. Phys. D **15**, 619 (2006).
- [41] R.H. Lin and X.H. Zhai, Phys. Rev. D **103**, 124001 (2021).
- [42] S.K. Maurya, et al., Fortschritte der Phys. **70**, 2200061 (2022).
- [43] M. Adak, T. Dereli, T.S. Koivisto and C. Pala, Int. J. Geom. Meth. Mod. Phys. **20**, 2350215 (2023).
- [44] W. Baade and F. Zwicky, Phys. Rev. **46**, 76 (1934).

- [45] M.S. Longair, *High Energy Astrophysics* (Cambridge Univeristy Press, Cambridge, 1994).
- [46] K. Dev and M. Gleiser, Gen. Relativ. Gravit. **39**, 1793 (2002).
- [47] M.K. Mak and T. Harko, Int. J. Mod. Phys. D **13**, 149 (2004).
- [48] M. Kalam, et al., Eur. Phys. J. C **72**, 2248 (2012).
- [49] F. Rahaman, et al., Eur. Phys. J. C **72**, 2071 (2012).
- [50] S.K. Maurya, et al., Phys. Rev. D **100**, 044014 (2019).
- [51] K.N. Singh, et al., Chin. Phys. C **44**, 105106 (2020).
- [52] P. Bhar, et al., Eur. Phys. J. C. **79**, 922 (2019).
- [53] M.K. Jasim, et al., Eur. Phys. J. C. **78**, 603 (2018).
- [54] J.H. Jeans, Mon. Not. R. Astron. Sot. **82**, 122 (1922).
- [55] J. Binney, Ann. Rev. Astron. Astrophys. **20**, 399 (1982).
- [56] G. Lemaitre, Ann. Sot. Sci. Bruxelles A **53**, 51 (1933).
- [57] R. Bowers and E. Liang, Astrophys. J. **188**, 657 (1974).
- [58] S. Bayin, Phys. Rev. D **26**, 1262 (1982).
- [59] L. Herrera and J. Ponce de Leon, J. Math. Phys. **26**, 2018 (1985).
- [60] L. Herrera and J. Ponce de Leon, J. Math. Phys. **26**, 2847 (1985).
- [61] K. Singh and K. Bhamra, Int. J. Theor. Phys. **29**, 1015 (1990).
- [62] M. Gokhroo and A. Mehra, Gen. Rel. Grav. **26**, 75 (1994).
- [63] H. Bondi, Mon. Not. R. Astron. Sot. **259**, 365 (1992).
- [64] L. Herrera and J. Ponce de Leon, J. Math. Phys. **26**, 2302 (1985).
- [65] L. Herrera and V. Varela, Phys. Lett. A **189**, 11 (1994).
- [66] L. Herrera, G. Ruggeri and L. Witten, Astrophys. J. **234**, 1094 (1979).

- [67] R. Chan, L. Herrera and N.O. Santos, *Class. Quantum Grav.* **9**, 133 (1992).
- [68] L. Herrera and N.O. Santos, *Phys. Report* **286**, 153 (1997).
- [69] R. Chan, L. Herrera and N.O. Santos, *Mon. Not. R. Astron. Soc.* **265**, 533 (1993).
- [70] L. Herrera, *Phys. Rev. D* **101**, 104024 (2020).
- [71] S.V. Lohakare, S.K. Maurya, K.N. Singh, B. Mishra and A. Errehymy, *Mon. Not. R. Astron. Soc.*, **526**, 3796 (2023).
- [72] S.K. Maurya, K.N. Singh, M. Govender, G. Mustafa and S. Ray, *Astrophys. J. Suppl. Ser.* **269**, 35 (2023).
- [73] S. Kaur, S.K. Maurya and S. Shukla, *Phys. Scr.*, **98**, 105304 (2023).
- [74] S.K. Maurya, et al., *Eur. Phys. J. C*, **83**, 18 (2023).
- [75] S.K. Maurya, et al., *Phys. Dark Universe*, **46**, 101619 (2024).
- [76] J. Kumar, et al., *Phys. Dark Universe*, **46**, 101593 (2024).
- [77] A. Errehymy, et al., *Phys. Dark Universe*, **46**, 101622 (2024).
- [78] S. Chaudhary, S.K. Maurya, J. Kumar and S. Ray, *Astropart. Phys.*, **162**, 103002 (2024).
- [79] S.K. Maurya, et al., *Class. Quantum Gravity*, **41**, 115009 (2024).
- [80] S.K. Maurya, et al., *Fortschr. Phys.*, **72**, 2300229 (2024).
- [81] G. Mustafa, A. Ditta, S. Mumtaz, S. S.K. Maurya and D. Sofuoglu, *Chin. J. Phys.*, **88**, 938 (2024).
- [82] Manzoor, R., et al.: *Eur. Phys. J. C* **79**(2019)831
- [83] Jawad, A., et al.: *Phys. Dark Universe*. **21** 70 (2018) .
- [84] Nawaz, T., Rani, S., Jawad, A.:*Chin. J. Phys.* **63**(2020)220
- [85] M.K. Jasim, D. Deb, S. Ray. Y.K. Gupta and S.R. Chowdhury, *Eur. Phys. J. C*, **78**, 603 (2018).

- [86] S. Biswas, D. Shee, S. Ray, F. Rahaman and B.K. Guha, *Ann. Phys.*, **409**, 167905 (2019).
- [87] M.F. Shamir and I. Fayyaz, *Int. J. Geom. Methods Mod. Phys.*, **17**, 2050140 (2020).
- [88] M.F. Shamir and T. Naz, *Phys. Dark Universe*, **27**, 100472 (2020).
- [89] P. Rej, P. Bhar and M. Govender, *Eur. Phys. J. C*, **81**, 316 (2021).
- [90] A. Ditta and T. Xia, *Chin. J. Phys.*, **79**, 57 (2022).
- [91] M. Bandyopadhyay and R. Biswas, *Phys. Lett. A*, **518**, 129676 (2024).
- [92] V. Singh and C.P. Singh, *Int. J. Theor. Phys.* **5**, 12571273 (2016).
- [93] D. Deb, et al., *Mon. Not. R. Astron. Soc.* **485**, 5652 (2019).
- [94] S. Biswas, et al., *Ann. Phys.* **409**, 167905 (2019).
- [95] M.F. Shamir, and T. Naz, *Phys. Dark Universe* **27**, 100472 (2020).
- [96] A. Majid and M. Sharif, *Universe* **6**, 124 (2020).
- [97] M. Javed, et al., *New Astron.* **84**, 101518 (2021).
- [98] S.K. Maurya, et al., *Phys. Rev. D* **100**, 044014 (2021).
- [99] J.B. Jimenez, L. Heisenberg and T. Koivisto, *Phys. Rev.* **98**, 044048 (2018).
- [100] R. Ferraro and F. Fiorini, *Phys. Rev. D* **84**, 083518 (2011).
- [101] V. Faraoni, *Phys. Rev. D* **81**, 044002 (2010).
- [102] P. Bhar, *Astrophys. Space Sci.* **354**, 457 (2014).
- [103] G. Abbas, S. Qaisar and M.A. Meraj, *Astrophys. Space Sci.* **357**, 042076 (2015).
- [104] G. Abbas, A.A. Kanwal and M. Zubair, *Astrophys. Space Sci.* **357**, 109 (2015).

- [105] R. Goswami, A.M. Nzioki, S.D. Maharaj and S.G. Ghosh, Phys. Rev. D **90**, 084011 (2014).
- [106] A. Cooney, S.D. Deo and D. Psaltis, Phys. Rev. D **82**, 064033 (2010).
- [107] A. Ganguly, R. Gannouji, R. Goswami and S. Ray, Phys. Rev. D **89**, 064019 (2014).
- [108] D. Momeni and R. Myrzakulov, Int. J. Geom. Methods Mod. Phys. **12**, 1550014 (2015).
- [109] A.V. Astashenok, S. Capozziello and S.D. Odintsov, J. Cosmol. Astropart. Phys. **12**, 040 (2013).
- [110] M.L. Rawls et al. Astrophys. J. **730**, 25 (2011).
- [111] F. Ozel, T. Guver and D. Psaltis, Astrophys. J. **693**, 1775 (2009).
- [112] H.A. Buchdahl, Phys. Rev. **116**, 1027 (1959).
- [113] M.K. Gokhroo and A.L. Mehra, Gen. Relativ. Gravit. **26**, 75 (1994).
- [114] L. Herrera, Phys. Lett. A **165**, 206 (1992).
- [115] S. Chandrasekhar, Astrophys. J. **14**, 417 (1964).